ISSN 1349-1113
JAXA-RR-08-003E

JAXA Research and Development Report

Thermophysical Properties of Liquid and Supercooled Rare Earth Elements Measured by an Electrostatic Levitator

Takehiko ISHIKAWA, Junpei T. OKADA, Jianqiang LI,
Paul-François PARADIS and Yuki WATANABE

February 2009

Japan Aerospace Exploration Agency

Thermophysical Properties of Liquid and Supercooled Rare Earth Elements Measured by an Electrostatic Levitator

By

Takehiko ISHIKAWA[*1], Junpei T. OKADA[*1], Jianqiang LI[*1,2],
Paul-François PARADIS[*1,3] and Yuki WATANABE[*4]

Abstract: Thermophysical properties of several rare earth elements have been measured using electrostatic levitation techniques. The understanding of the nature and behavior of rare earth metals in their liquid phases requires accurate values of their physical properties. However, keeping the samples in their liquid phases free from contamination long enough to carry out measurements represents a formidable challenge. This is due to the high reactivity and contamination of these elements with a crucible or with a gaseous environment. The use of an electrostatic levitator in vacuum circumvents these difficulties and permits the measurements of the density, the surface tension, and the viscosity of these metals above and below their melting temperature. In this paper, the measurement methods as well as the levitation apparatus are introduced and the measured values are reported.

Keywords: rare earth elements, liquid, density, surface tension, viscosity

1. INTRODUCTION

Rare earth elements and their compounds are currently used to improve the resistance of certain glasses, to fabricate hydrogen sponges and strong magnets, and as dopants in optical amplifiers[1)]. To assist further material development, the knowledge of the physical properties of rare earth metals and their temperature dependences is therefore paramount. However, rare earths are very reactive, oxidizing rapidly when exposed to air and reacting directly with nitrogen and other elements[1)].

This explains why accurate physical properties are difficult to measure above their melting points when traditional methods are used (e.g., crucible, support) and why there are no data reported in the supercooled region. Here, an electrostatic levitator in vacuum isolated a sample against contaminating walls and surrounding gases[2-5)]. This circumvented the problems related to high temperature processing and allowed an accurate non-contact determination of the density, the surface tension, and the viscosity of liquid Y, La, Ce, Pr, Nd, Gd, Tb, and Lu. This paper shortly introduces the facility, describes the processing and property determination methods, and then presents preliminary experimental results.

2. EXPERIMENTAL SETUP AND PROCEDURES

2.1. Electrostatic Levitator

The measurements were made using an electrostatic levitator (Fig. 1)[2)] which consisted of a chamber evacuated to a ~10^{-5} Pa vacuum level before processing was initiated. The chamber housed a sample charged by electronic emission and levitated between electrodes via a

＊1 Japan Aerospace Exploration Agency, 2-1-1 Sengen, Tsukuba, Ibaraki, 305-8505 Japan.
＊2 Institute of Process Engineering, Chinese Academy of Sciences, P.O. Box 353, Beijing, 100190, P. R. China.
＊3 Mitsubishi Materials Co., 1002-14 Mukoyama, Naka, Ibaraki, 311-0102 Japan.
＊4 Advanced Engineering Services Co. Ltd.,1-6-1 Takezono, Tsukuba, Ibaraki, Japan.

feedback loop. The two disk electrodes were used for the vertical position control whereas four spherical electrodes were dedicated to horizontal control[6]. The positioning control relied on two sets of orthogonally arranged He-Ne lasers and the associated position detectors. The three dimensional sample position information was fed to a computer that generated and sent appropriate *x*, *y*, and z position control signals to high voltage amplifiers so that a prefixed sample position could be maintained. The lower electrode was surrounded by four coils that generated a rotating magnetic field that was used for rotation control[7]. Specimens were prepared by arc melting powder or chunks of materials into spheroids with diameters of around 2 mm. The purity of each element is listed in Table-1.

Three laser beams were used for sample heating (Fig. 1). The beam of one CO_2 laser (10.6 μm emission) was sent directly to the sample whereas that from another CO_2 laser was divided into two beams such that the three focused beams in a same plane, separated by 120 degrees, hit the specimen. This configuration provided temperature homogeneity, improved sample position stability, and helped to control sample rotation.

The radiance temperature was measured with a single-color pyrometer (0.90 μm, 120Hz acquisition rate) covering a 900 to 3800 K interval. The temperature was calibrated to true temperature using the melting plateau of the sample.

The sample was observed by three charge-coupled-device (CCD) cameras. One color camera offered a view of both the electrodes and the sample whereas two black and white high-resolution cameras (camera-1 and camera-2), located at right angles from each other and equipped with telephoto objectives, provided magnified views of the sample for density measurements. This also helped to monitor the sample position in the horizontal plane and to align the heating laser beams to minimize photon-induced horizontal sample motion and sample rotation[8].

Table 1 Information of rare earth samples used in electrostatic levitation experiments

	Melting Temperature (K)	Purity (mass %)	Shape	Manufacturer
Y	1796	99.9	Powder	Nilaco
La	1191	99.9	Rod	Nilaco
Ce	1072	99.9	Ingot	*
Pr	1204	99.9	Rod	Nilaco
Nd	1294	99.9	Rod	Nilaco
Gd	1586	99.9	Rod	Nilaco
Tb	1629	99.9	Foil	Nilaco
Lu	1936	99.9	Rod	Nilaco

* Beijing Mountain Technical Development Center for Non-ferrous metals

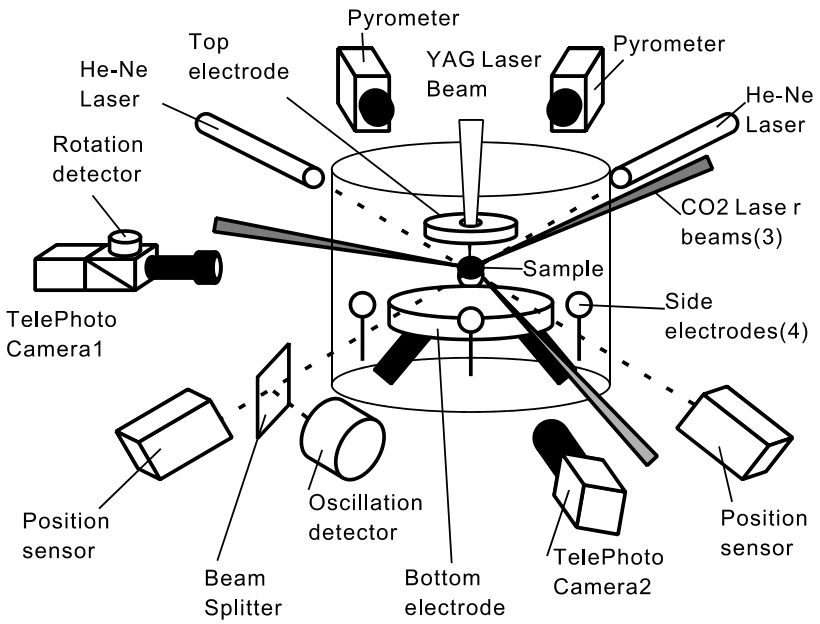

Fig. 1 Schematic view of the electrostatic levitation furnace and its diagnostic apparatus.

2.2. Thermophysical Property Determination

Density measurements were carried out using a UV imaging technique described in detail elsewhere[4,9]. First, a solid sample was levitated and rotation about the vertical-axis was induced by a rotating magnetic field. The rotation rate of the solid sample was measured by a detector, which monitored the intensity of He-Ne lasers reflected from the uneven sample surface[7]. When the rotation rate reached 10 Hz, the rotating magnetic field was turned off. All CO_2 laser beams were directed in such a way to minimize photon-induced rotation during the sample heating. Once a levitated sample was melted, it became spherical due to surface tension and the distribution of surface charge. If the shape of a molten sample departed from that of a sphere (due to excessive rotation), a counter torque was applied by the magnetic field to restore the spherical shape. The controlled sample rotation not only improved the temperature homogeneity of the sample, but also prevented precession and ensured to maintain the axi-symmetry of the sample along the vertical axis.

Images at the rate of 30 frames/s and temperature data were simultaneously recorded as a function of time. All laser beams were then blocked with mechanical shutters allowing the sample to cool radiatively. After the experiment, the video images from one high-resolution camera were digitized. Since the sample was axi-symmetric, the sample volume (V) could be calculated from each image. The recorded images were calibrated by levitating a stainless steel sphere with a precisely known radius under identical experimental conditions. The images were then matched with the thermal history of the sample (Fig. 2). Because the mass of the sample (m) was known, the density could be determined as a function of temperature with the following equation:

$$\rho = m / V \ . \tag{1}$$

Although the sample evaporated as evidenced by a change in radius during long levitation periods (hours), the density experiments lasted only a few minutes, for which the melting temperature was exceeded for only a few seconds (Fig. 2). Therefore, the effect on density was negligible.

The surface tension and the viscosity were determined by the oscillating drop method[10]. In this method, a solid sample was first levitated, rotated to ~10 Hz, heated, melted, and brought to a selected temperature. Then, a P_2 ($\cos\theta$)-mode drop oscillation was induced to the sample by superimposing a small sinusoidal electric field on the levitation field. One of the positioning He-Ne laser beams was divided by a beam splitter and lead to an oscillation detector, which consisted of a power detector and a vertical slit. The shadow of the levitated sample was projected on this detector and variation of the vertical diameter of the sample was translated to an electrical signal. The transient signal that followed the termination of the excitation field was detected and analyzed using a custom-made program. This was done several times at a given temperature and repeated for several temperatures. Using the characteristic oscillation frequency ω_c of the signal, which was calculated by a fast Fourier transform (FFT) analysis and then corrected for non uniform surface charge distribution, the surface tension γ could be determined from[11]:

$$\omega_c^{\ 2} = \left(\frac{8\gamma}{\rho r_0^{\ 3}} \right) Y, \tag{2}$$

where r_0 is the radius of the sample, ρ is the density, and Y is the correction factor that depends on the drop charge, the permittivity of vacuum, and the applied electric field[12,13]. Similarly, using the decay time τ given by the same signal, the viscosity η could be determined by

$$\eta = \frac{\rho r_0^2}{5\tau} \ .^{14)} \tag{3}$$

During the experiments, the video images from a high-resolution camera were recorded. After the experiment, each value of the radius at each oscillation was obtained by image analysis. This procedure eliminated the measurement error due to sample evaporation. Moreover, the aspect ratio of the sample (ratio between the horizontal and vertical radii) was also calculated to evaluate the experimental error induced by sample rotation.

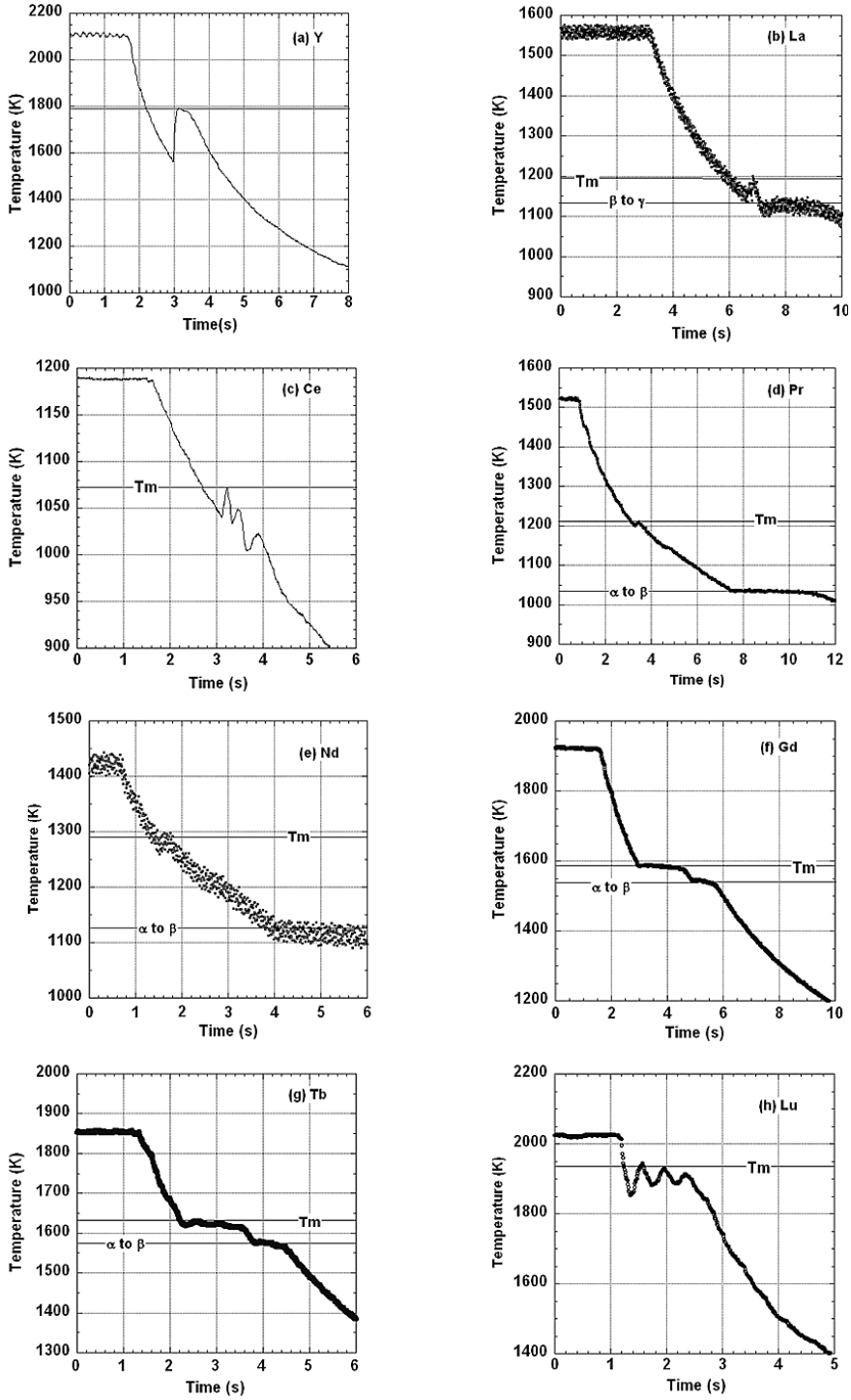

Fig. 2 Radiative temperature profiles for molten rare earths samples: (a)Y, (b) La, (c) Ce, (d) Pr, (e) Nd, (f) Gd, (g) Tb, and (h) Lu.

2.3. Experimental Uncertainties

The experimental uncertainty for density measurements was derived from the respective uncertainty measurements for the mass and volume of samples. Because the uncertainty in mass was 0.1 mg while a typical sample mass was around 30 mg, the uncertainty can be estimated to be around 0.3 %. The uncertainty of volume ($\Delta V/V$) could be calculated by

$$\frac{\Delta V}{V} = \frac{3\Delta r_0}{r_0} \tag{4}$$

where Δr_0 is the uncertainty in radius measurement by the image analysis[9]. In our experiment, the average value of Δr_0 was around 1 pixel, while r_0 was 160 pixels. Therefore, $\Delta V/V$ can be estimated to be around 1.9%, and the overall uncertainty of density measurement ($\Delta\rho/\rho$) was estimated to be about 2%.

Based on equation (2), the uncertainty in surface tension measurement was mainly determined by those of ρ, r_0, and ω_c As described earlier, the uncertainty of ρ and r_0 were 2 % and 0.65 %, respectively. The uncertainty of ω_c induced by the FFT analysis was negligibly small (0.4 %) and evaluated by considering the transformation error (less than 1 Hz) and the typical characteristic oscillation frequency (around 250 Hz). As a result, the uncertainty of the surface tension measurements ($\Delta\gamma/\gamma$) could be estimated to be around 3 % by the following equation:

$$\frac{\Delta\gamma}{\gamma} \approx \sqrt{\left(\frac{\Delta\rho}{\rho}\right)^2 + \left(\frac{3\Delta r_0}{r_0}\right)^2 + \left(\frac{\Delta\omega_c}{\omega_c}\right)^2} \tag{5}$$

Similarly, the uncertainty of viscosity measurement could be estimated by the uncertainties of ρ, r_0, and τ. The uncertainty of the decay time $\Delta\tau$ was estimated to be about 15 %, which was due mainly to the sample motion with respect to the detector during drop oscillation. This determined the overall uncertainty of viscosity.

3. RESULTS AND DISCUSSIONS

3.1. Density

As shown in figures 2, upon closing the shutters of all heating lasers, samples of all elements (Y, La, Ce, Pr, Nd, Gd, Tb, and Lu) exhibited slight supercooling, liquid-solid transition, as well as allotropic transitions (La: fcc to bcc, 1134 K; Nd: cph to bcc, 1128 K)[15]. The density measurements of liquid yttrium, lanthanum, cerium, praseodymium, neodymium, gadolinium, terbium, and lutetium are shown in Fig. 3. Other rare earth elements (e.g.,.Sm, Eu, Dy, Ho, Er, Tm, and Yb) could not melt under high vacuum due to their high vapor pressure.

These density data, like those of other pure metals, exhibited a linear behavior as a function of temperature. The measured data and reference values are listed in Table-2. The volume expansion coefficients at the melting temperature (β_m) were calculated with the following formula:

$$\beta = -\frac{1}{\rho} \bullet \frac{d\rho}{dT} \tag{6}$$

A simple relationship between the temperature dependence of the density of liquid metals and their boiling temperatures (T_b) was proposed by Steinberg[22]. He collected liquid density data at the melting point and the temperature dependence of liquid density for 44 elements and found the following empirical relation:

$$-\frac{d\rho}{dT} \propto \frac{\rho_{00}}{T_b} \tag{7}$$

where ρ_{00} was the virtual density of the liquid at 0 K, determined by extrapolation from ρ_m and T_m with:

$$\rho_{00} = \rho_m - \frac{d\rho}{dT} T_m \tag{8}$$

Figure 4 illustrates the correlation of $-d\rho/dT$ with ρ_{00}/T_b. In this study, most of the metal elements followed this correlation. In Fig.4, our measured data of refractory metals[23-27] and those of rare earth elements were also plotted. Our data for the rare earths, except that for cerium, showed a good agreement with Steinberg's relation.

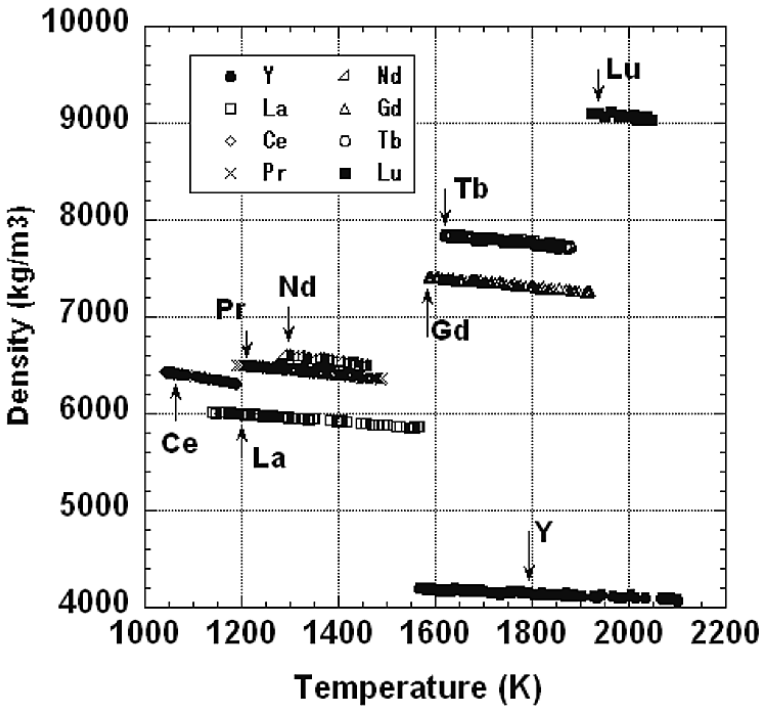

Fig. 3 Density of liquid rare earth elements versus temperature

3.2. Surface Tension

Figure 5 depicts the results for the surface tension of rare earths as a function of temperature. Like the density data, the surface tension data show a linear temperature dependence. Table-3 summarizes our measurements the literature values. Because the rare earth elements are very easily oxidized, surface tension measurements in the supercooled region were very hard to perform. Improvement of the vacuum level is necessary to obtain data in this region.

When considering the experimental uncertainties, our results at the melting temperature show excellent agreement with the works of Chentsov[29] and Bezukladnikova *et al*.[30] (La) and those of Bezukladnikova *et al*.[30] (Pr). For Ce, Nd, and Tb, our results were systematically higher than the literature data. The lower surface tension data reported elsewhere could be explained by the fact that the measurements were done with techniques for which a contact between a molten sample and a surface (e.g., sessile drop technique) occurred, which is not the case with our technique. The contact could have further contaminated the surface of the sample and therefore lowered the surface tension[37]. Additional surface contamination could have occurred for samples that were processed under non-high vacuum conditions because of the oxygen and nitrogen affinity of those rare earths[1].

It is well known that the surface tension at the melting temperature (γ_m) shows a good correlation with the following function[17,37]:

$$\gamma_m \propto \frac{RT_m}{V_m^{2/3}} \tag{9}$$

where R is the gas constant (8.31 J.mol^{-1}·K^{-1}) and V_m is the molar volume at the melting temperature. Fig.6 depicts the correlation between γ_m and (RT_m $(V_m)^{-2/3}$) for 57 elemental metals[38]. Our measurement data of rare earths as well as other refractory metals showed a good agreement with equation (9).

Compared with refractory metals, temperature coefficients of rare earths are small (less than -0.1 mNm^{-1}K^{-1}). The literature values for Nd and La agree with our data. However, our data for Pr and Tb were respectively around 50% smaller and 70% higher than those of the literature. Kasama *et al*.[39] proposed an empirical equation based on a physical model. Based on this model, the surface tension and its temperature dependence can be expressed as:

Table 2 Present work and literature values for the density of liquid rare earths.

	ρ^{TM} (kgm^{-3})	$d\rho/dT$ (kgm^{-3}K^{-1})	Temperature Range (K)	Volume expansion coefficient $\beta(T_m)$ (10^{-5}K^{-1})	Reference
Y	4150 ± 30	-0.21 ± 0.02	1560-2100	5.1	Present work
	4150				Fogel[16]
	4180	-0.29	1795-1958		Kononenko[17]
	4390				Kononenko[17]
	4143				Kononenko[17]
La	6001 ± 16	-0.39 ± 0.01	1140-1570	6.4	Present work
	5957	-0.237	1224-1277	3.9	Wittenberg[18]
	5955	-0.242		4.1	Wittenberg[18]
	5940	-0.61	1191-1873	10.3	Kononenko[17]
Ce	6409 ± 31	-0.83 ± 0.03	1040-1190	12.9	Present work
	6550	-0.7	1081-1730		Kononenko[17]
	6690				Kononenko[17]
Pr	6500 ± 9	-0.51 ± 0.01	1190-1490	7.8	Present work
	6611	-0.24	1210-1278	3.6	Wittenberg[18], Eichelberger[19]
	6500	-0.93	1204-1730	14.3	Kononenko[17]
Nd	6585 ± 55	-0.57 ± 0.04	1280-1460	8.7	Present work
	6890	-0.76	1294-1630	11.3	Kononenko[17]
	6688	-0.528	1294-1520	7.9	Rohr[20]
Gd	7410 ± 44	-0.46 ± 0.03	1586-1920	6.2	Present work
	7790	-1.00	1584-1830		Kononenko[17]
	6910				Kononenko[17]
	7404				Kononenko[17]
Tb	7839 ± 39	-0.47 ± 0.02	1615-1880	6.1	Present work
	7679	-0.48	1629-1780	6.3	Stankus[21]
	8050	-1.39	1629-1780	17.3	Kononenko[17]
Lu	9100	-0.52	1923-2037	5.7	Present work
	9750	-2.04	1925-2020		Kononenko[17]

$$\gamma = \frac{1}{2}\frac{\pi^2 C^2 \delta^2 T_m}{N_A M^{2/3}}\left(\frac{\rho}{\rho_m}\right)^{2/3}\left\{(\alpha+1)\rho^{1/3} - \rho_m^{1/3}\right\}^2$$
$$\frac{d\gamma}{dT} = -\frac{1}{3}\frac{\pi^2 C^2}{N_A}\frac{T_m \Lambda \delta^2}{M^{2/3}}\left\{2(\alpha+1)^2\rho^{1/3}\rho_m^{2/3} + \rho^{-1/3} - 3(1+\alpha)\rho_m^{-1/3}\right\} \quad (10)$$

where N_A was Avogadro's number, M was the atomic number, Λ was the temperature dependence of density ($-d\rho/dT$), C was a constant derived from Lindemann's theory of melting (ranged from 2.8 x 10^{12} to 3.1 x 10^{12}), δ was the ratio between the characteristic vibration frequency in the liquid phase and the solid phase (estimated to be around 0.5), and α was a constant indicating the distance where an attractive force by an atom was effective (ranged from 0.45 to 0.65).

At the melting temperature, the temperature coefficient of the surface tension could be calculated by

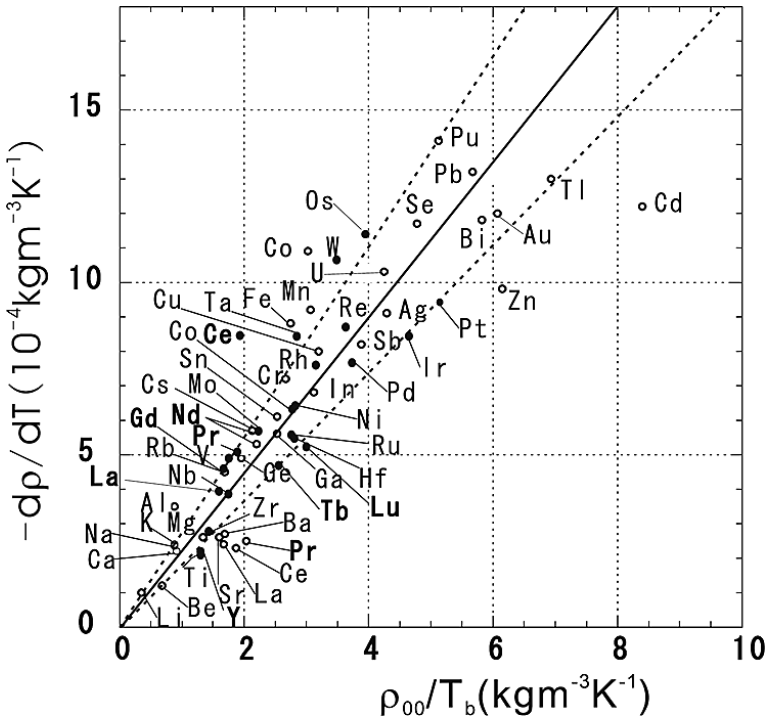

Fig. 4 Correlation of $d\rho/dT$ with ρ_{00}/T_b for the elements. Open and black circles represent data from Ref. 21 and data measured by an electrostatic levitator, respectively. The solid line is the best fit to the data and the dashed lines represent the 20% error cone from Ref. 22.

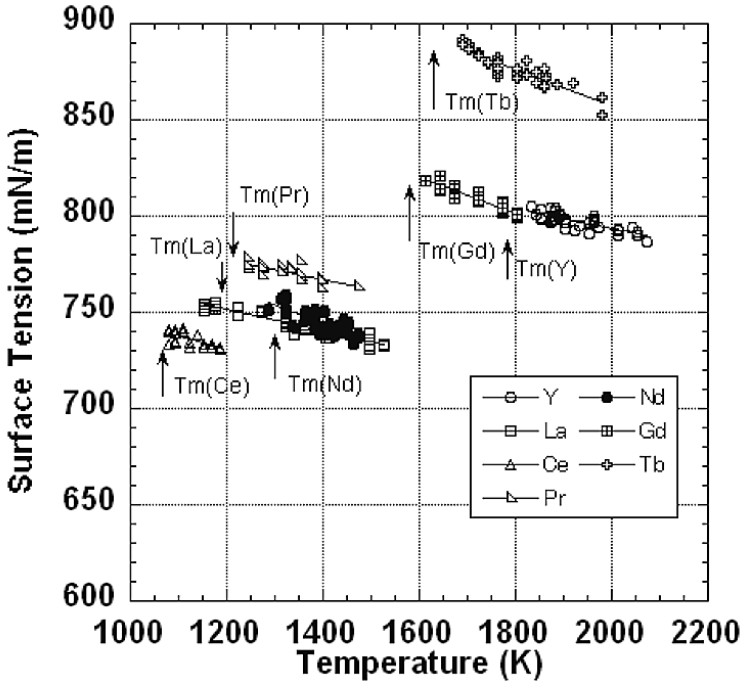

Fig. 5 Surface tension of rare earth elements versus temperature.

$$\frac{d\gamma}{dT} = -\frac{1}{3}\frac{\pi^2 C^2}{N_A}\frac{T_m \Lambda \delta^2}{M^{2/3}}\rho_m^{-1/3}\left(2\alpha^2 + \alpha\right) \tag{11}$$

In this formula, the uncertainties of the constants (C, α, and δ) seriously affected the temperature dependence of the surface tension. Two of those constants could be eliminated by combining equations (10) and (11), and the temperature coefficient of the surface tension could

be determined as

$$\frac{d\gamma}{dT} = -\frac{2}{3}\frac{\Lambda\gamma_m}{\rho_m}\frac{2\alpha+1}{\alpha} = K\frac{\Lambda\gamma_m}{\rho_m} = K\gamma_m\beta_m$$
$$K \equiv \frac{-2(2\alpha+1)}{3\alpha} \tag{12}$$

Table 3 Present work and literature values of the surface tension for liquid rare earths.

	$\gamma(T_m)$ (10^{-3}Nm^{-1})	$d\gamma/dT$ (10^{-3}Nm^{-1}K^{-1})	Temperature Range (K)	Reference
Y	804 ± 33	-0.05 ± 0.02	1830-2070	Present work
	872	-0.086		Kononenko[17]
	870 ± 12	-0.086	1795-1958	Allen[28]
La	752 ± 9	-0.056 ± 0.007	1150-1525	Present work
	745	-0.10	1191-1650	Chentsov[29]
	739	-0.106	1191-1620	Bezukladnikova[30]
	729	-0.098	1191-1750	Sukhman[31]
	728	-0.10	1191-1873	Kononenko[17]
	701		1191	Martsenyuk[32]
	700		1191	Kingery[33]
	720	-0.32		Pulliam[34]
Ce	751 ± 36	-0.07 ± 0.03	1079-1185	Present work
	707	-0.078	1081-1730	Kononenko[17]
	740			Allen[28]
Pr	777 ± 29	-0.052 ± 0.02	1240-1475	Present work
	690	-0.073	1204-1730	Kononenko[17]
	690	-0.071	1204-1800	Sukhman[31]
	723		1204	Martsenyuk[32]
	743	-0.092	1204-1873	Bezukladnikova[30]
	706	-0.080	1204-1873	Chentsov[29]
Nd	754 ± 25	-0.095 ± 0.018	1290-1475	Present work
	685	-0.07	1289-1630	Kononenko[17]
	685	-0.087	1289-1630	Sukhman[31]
	688		1294	Lasarev[35]
	689	-0.09		Lasarev[36]
Gd	822 ± 33	-0.097 ± 0.02	1613-1803	Present work
	664	-0.058	1584-1830	Kononenko[17]
	810			Allen[28]
Tb	823 ± 28	-0.096 ± 0.015	1690-1980	Present work
	700		1629	Fogel[16]
	669	-0.056	1629-1780	Sukhman[29]

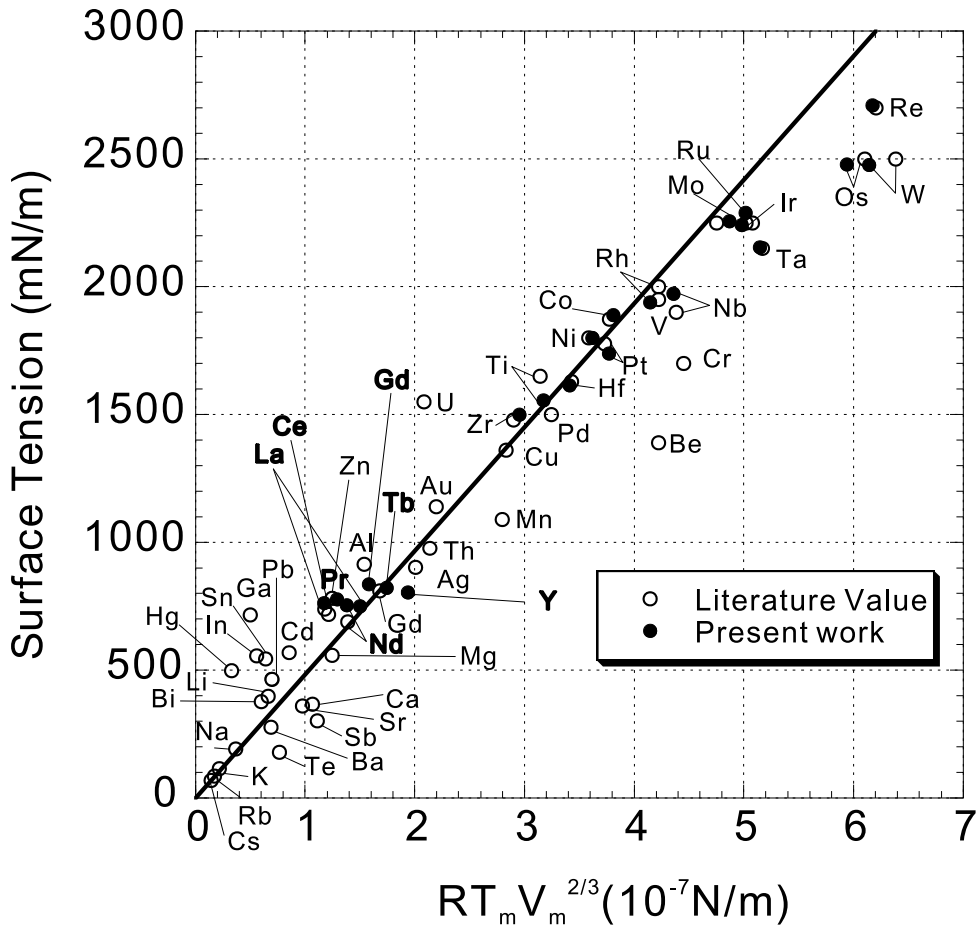

Fig. 6 Correlation of surface tension at the melting temperature (γ_m) with ($RT_m/V_m^{2/3}$) for various liquid metals.

This equation suggested that the temperature dependence of the surface tension was proportional to the product of the surface tension at the melting temperature by the thermal expansion coefficient. Validity of this formula for liquid metals was checked using the literature data[40-42] and our measurements obtained with the electrostatic levitator (ESL)[43-45]. The results are shown in figure 7.

Literature data for alkaline metals showed good agreements with equation (12), while those for transition metals exhibit scatter, some being far from the relation. Particularly, data for lanthanum is far out of the proposed correlation. However, the data measured by ESL exhibited the same tendency as those of the alkaline metals (except Ce). Based on the ESL results, the temperature dependence of the surface tension of metal elements could be estimated if the surface tension at the melting temperature and if the thermal expansion coefficient were known.

3.3. Viscosity

Figure 8 illustrates our viscosity data that could be fitted by the following Arrhenius function:

$$\eta(T)=\eta_0\exp(E/RT) \tag{13}$$

where R is the gas constant (8.31 $J.mol^{-1}\cdot K^{-1}$), η_0 is the pre-exponential viscosity, and E is the activation energy. Values of η_0 and E are listed in Table-4 together with literature values. The scatter observed in the data is mainly due to the motion of the sample with respect to the oscillation detector. No other experimental values were found for Nd, Gd and Tb.

The most successful quantitative correlation between the viscosity of liquid metals and other thermophysical properties is that of Andrade[49]. Andrade obtained the following formula by assuming that the characteristic vibration frequency in the liquid at the melting point is equal to that in the solid, which can be estimated from the Lindemann's law[50]:

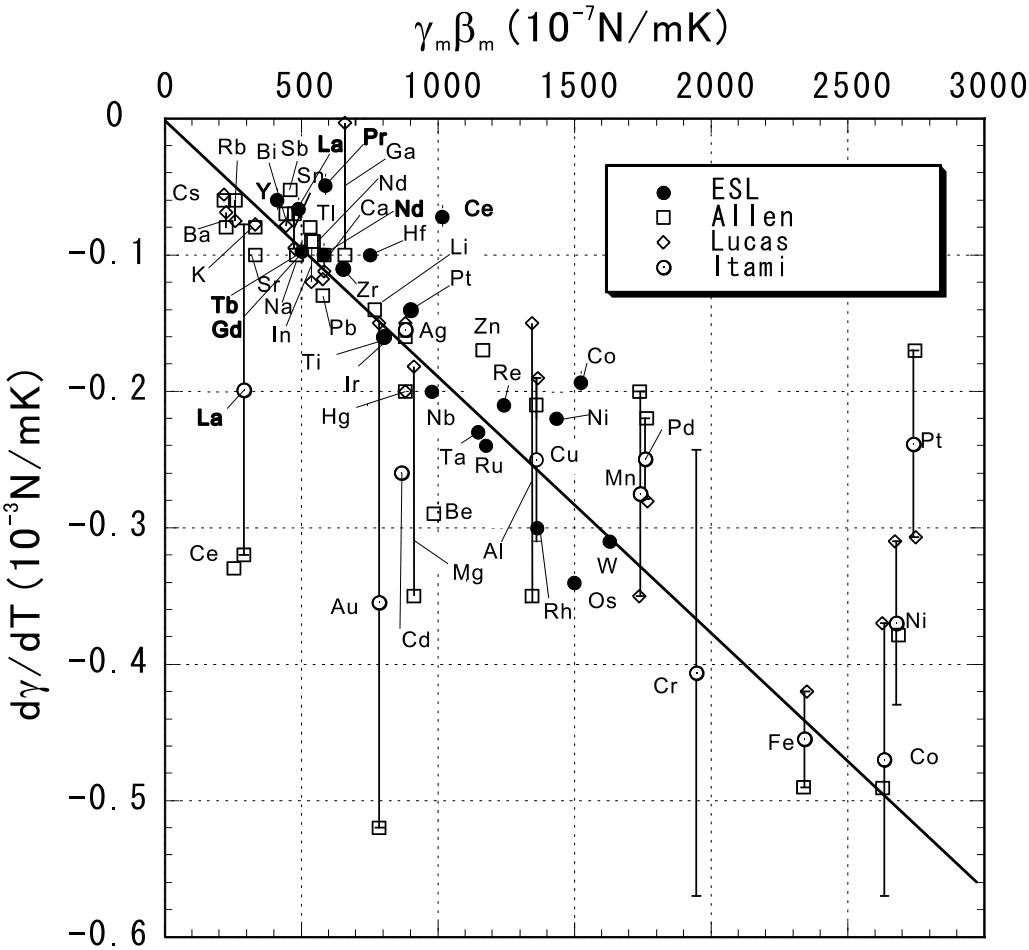

Fig. 7 Correlation between $\gamma_m\beta_m$ and $d\gamma/d\mathbf{T}$

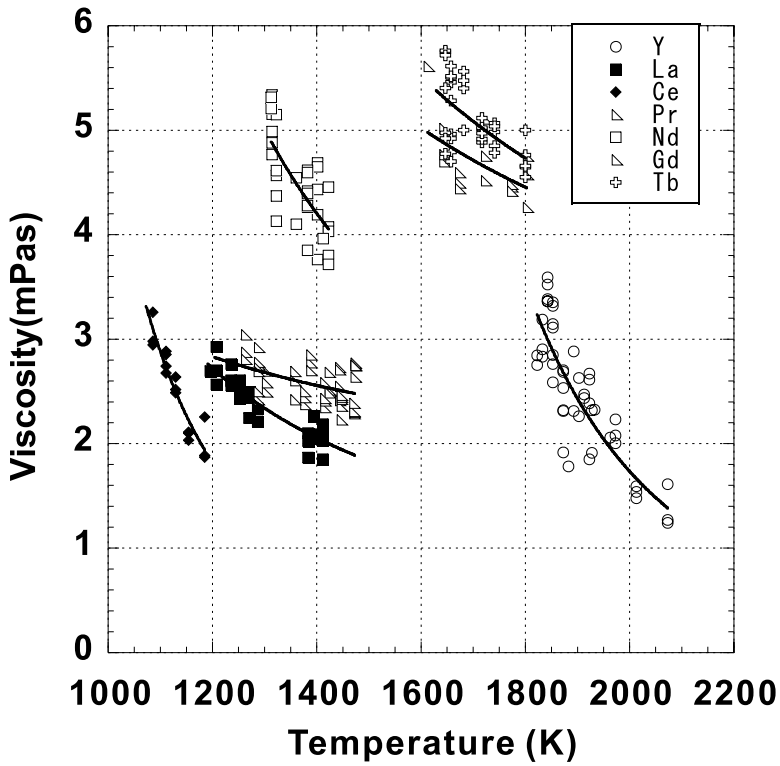

Fig. 8 Viscosity of rare earth metals versus temperature.

Table 4 Present work and literature values of the viscosity of liquid rare earths.

	$\eta(T_m)$ (mPa·s)	$\eta(T)=\eta_0\exp(E/RT)$		Temperature Range (K)	Reference
		η_0 (mPa·s)	E (kJ·mol^{-1})		
Y	3.6	0.00287	106.5	1830-2070	Present work
La	2.75	0.381	19.6	1195-1410	Present work
	2.45	0.209	25.2	1191	Wittenberg[46]
	3.13	0.2317	26.255	1213-1493	Frohberg[47]
	2.65				Iida[38]
Ce	3.31	0.012	50.5	1086-1185	Present work
	2.88				Wittenberg[48]
Pr	2.82	1.38	7.14	1260-1475	Present work
	2.80	0.936	11.2	1204-1280	Wittenberg[48]
	2.80	1.758	4.678		Lucas[39]
	2.85				Iida[38]
Nd	5.07	0.43	26.5	1310-1420	Present work
Gd	4.9	1.7	14	1613-1803	Present work
Tb	5.3	1.399	18.2	1647-1800	Present work

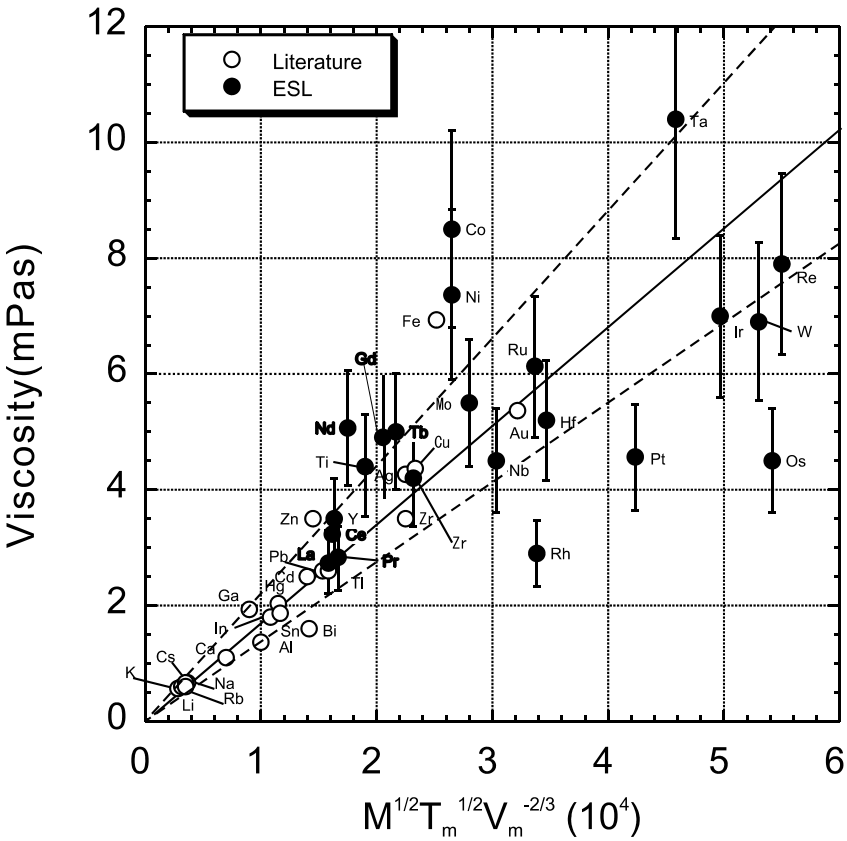

Fig. 9 Correlation between $M^{1/2}T_m^{1/2}V^{-2/3}$ and viscosity based on Andrade's formula. Measured values by ESL (black circle) are shown with 20% error bar.

$$\eta(T_m) = CA\frac{\sqrt{MT_m}}{V_m^{2/3}}. \tag{14}$$

where M is the atomic mass. Fig.9 illustrates the validity of the Andrade's formula with the data measured by ESL and data found in the literature. Except for Nd, the viscosity of rare earth metals shows a good agreement with the formula. The current uncertainty of viscosity measurement is at least 20%. Improvement of viscosity measurement is necessary to quantitatively evaluate the validity of Andrade's formula.

4. CONCLUSIONS

The density, the surface tension, and the viscosity of several rare earth metals were measured with an electrostatic levitator. The containerless processing and non-contact measurement techniques eliminated contamination from a crucible as well as suppressed nucleation at the melting temperature. This enabled the measurement of the thermophysical properties over wide temperature ranges. The measured data of rare earth metals, coupled with other refractory metals data, were compared with the literature values as well as estimated data based on several correlation formulae.

Acknowledgments

This work was supported by a Grant-in-Aid for Scientific Research (B) from the Japan Society for the Promotion of Science. One of the authors (JQL) wished to acknowledge the support from the National Natural Science Foundation of China (No. 50704031).

REFERENCES

1. D. R. Lide and H. P. R. Frederikse: *CRC Handbook of Chemistry and Physics*, (CRC Press, Boca Raton, Florida, 1997) 78th ed.
2. P.-F. Paradis, T. Ishikawa, and S. Yoda: ESA **SP–454** (2001), 993.
3. T. Ishikawa, P.-F. Paradis, and S. Yoda, *J. Jpn*. Soc. Microg. *Appl.* **18** (2001), 106.
4. T. Ishikawa, P.-F. Paradis, and S. Yoda: *Rev. Sci. Instrum*. **72** (2001), 2490.
5. P. –F. Paradis, T., Ishikawa, and S. Yoda, *Int. J. Thermophys.,* **23**, (2002), 825.
6. W.-K. Rhim, S. -K. Chung, D. Barber, K.-F. Man, G. Gutt, A. A. Rulison, and R. E. Spjut, *Rev. Sci. Instrum*. **64** (1993) 2961.
7. W.-K. Rhim and T. Ishikawa, *Rev. Sci. Instrum*. **69** (1998) 3628.
8. W.-K. Rhim and P.-F. Paradis, *Rev. Sci. Instrum*. **70** (1999) 4652.
9. S.-K. Chung, D. B. Thiessen, and W.-K. Rhim, *Rev. Sci. Instrum*. **67** (1996) 3175.
10. W.-K. Rhim, K. Ohsaka, P.-F. Paradis, and R. E. Spjut, *Rev. Sci. Instrum*. **70** (1999), 2996.
11. Lord Rayleigh, *Proc. R. Soc. London* **29** (1879), 71.
12. Lord Rayleigh, *Philos. Mag*. **14** (1882), 184.
13. J. Q. Feng and K. V. Beard, *Proc. R. Soc. London A* **430** (1990), 133.
14. H. Lamb, *Hydrodynamics* (Cambridge University Press, 1932) 6th ed., 473.
15. A. T. Dinsdale, *CALPHAD*, **15**, (1991), 317.
16. A. A. Fogel, T. A. Sidorova, G. E. Chuprikov, M. M. Mezdrogina, *Izv. Akad. Nauk SSSR Metal*., **1** (1965), 50.
17. V. I. Kononenko, A. L. Sukhman, S. L. Gruverman, and V. V. Torokin, *Phys. Stat. Solid*., **84A**, (1983), 423.
18. L. J. Wittenberg, D. Ofte, and W.G. Rohr, "Rare Earth Research", Vol II ed. K.S. Vorres, Gordon and Breach, (1964), 257.
19. J. F. Eichelberger, Mound Lab. Rep. 1118, (1961), 12.
20. W. G. Rohr, *J. Less Common Metals*, **10**, (1966), 389.
21. S. V. Stankus, A. S. Basin, Tezisi. VII vsesoyuznoi konf. Teplofizicheskie svoistvaveschestv, chap. 2, Inst. Teplofiz. Sov., AN SSSR (in Russian), Novosibirsk (1982), 80.
22. D. J. Steinberg, *Metallurgical Transactions* **5** (1974), 1341.
23. T. Ishikawa, P. –F. Paradis, T. Itami, and S. Yoda, *Meas. Sci. Technol*. **16** (2005), 443.
24. T.Ishikawa and P.-F. Paradis, *Journal of Electronic Materials*, **34** (2005), 1526.
25. P. -F. Paradis, T. Ishikawa, R. Fujii, and S. Yoda, *Appl. Phys. Lett*. **86** (2005), 41901.
26. T. Ishikawa, P. –F. Paradis, and N. Koike, *JJAP* **45** (2006), 1719.
27. P.-F. Paradis,T. Ishiakwa, and N. Koike, *JAP* **100** (2006), 103523.
28. B.C. Allen, in "Liquid Metals, Chemistry and Physics", Ed. S. Z. Beer. M. Dekker Inc. New York 1972, 161.

29. V. P. Chentsov, Dissertation Inst. Tekh. Metallurgiya UNTs, Akad. Nauk. SSSR, Sverdlovsk, 1972.
30. L. L. Bezukladnikova, V. I. Kononenko, V.V. Torokin, *Teplofiz. Vys. Temp*., **27**, (1989), 478.
31. A. L. Sukhman, V. I. Kononenko, S. L. Gruverman, and V. V. Torokiv, Poverkhnostnye svoistva rasplavov (Surface properties of melts) (in Russian), 107, Nauka Dumka, 1982.
32. P. S. Martsenyuk, and Y. N. Ivashchenko, *Adgez. Rasp. Paika Mate*r., **19**, (1984), 12.
33. W. D. Kingery, *Amer. Ceram. Soc. Bull*., **35**, (1956), 108.
34. G. R. Pulliam, and E. S. Fitzsimmons, Report US Atom. Energy Comm, Ames Lab. Rep. No.ISC-659-1955, 1955.
35. A. Lasarev and I. V. Pershikov, *Dokaldy A.N*., **146**, (1962), 143.
36. V. B. Lasarev and A. V. Pershikov, *Proc. Acad. Sci. USSR, Phys. Chem. Sect*. **146**, (1962), 637.
37. B. J. Keene, “Surface Tension of Pure Metals”, National Physical Laboratory, Publication DMM (A) 39, 1991.
38. T. Iida and R. I. L. Guthrie: *The Physical Properties of Liquid Metals*, (Clarendon Press, Oxford 1988).
39. A. Kasama, T. Iida, and Z. Morita, J. *Japan Inst. Metals*, **40** (1976), 1030.
40. B. C. Allen, Trans. AIME **227** (1963), 1175.
41. L. D. Lucas, *Tech l’Ing.,* **7**, Form. M65 (1984).
42. T. Itami, in *Condensed Matter Disordered Solids*, ed. S. K. Srivastava and N. H. March (World Scientific. 1995), Chap.3
43. T. Ishikawa, P. –F. Paradis, T. Itami, and S. Yoda, *JAXA Research and Development Report*, JAXA-RR-04-024E (2005).
44. T. Ishikawa, P. –F. Paradis, and N. Koike, *JAXA Research and Development Report*, JAXA-RR-05-015E (2006).
45. T. Ishikawa, P. –F. Paradis, and N. Koike, *JAXA Research and Development Report*, JAXA-RR-06-012E (2007).
46. L. J. Wittenberg and R. DeWitt, in *The properties of Liquid Metals*, (ed. by S. Takeuchi), Taylor & Francis, London (1973), 555.
47. M. Frohberg and T. Cakici, *Z. Metallkunde*, **69**, (1978), 296.
48. L. Battezzati and A. L. Greer, *Acta Metall*. **37** (1989), 1791.
49. E. N. Da C. Andrade, *Phil. Mag*. **17** (1934), 497.
50. F. A. Lindemann, *Phys. Z.* **11** (1910), 609.